

Gluon Polarization from correlated high- p_T hadron pairs in polarized electro-production

Alessandro Bravar*, Dietrich von Harrach, and Aram Kotzinian†

Institut für Kernphysik, Universität Mainz, D-55099 Mainz, Germany

October 17, 2018

Abstract

We propose to measure the polarized gluon distribution function $\Delta G(\eta)$ at $\eta \lesssim 0.2$ via *pseudo* jet production in polarized fixed target lepton nucleon scattering at typical lepton beam energies of 200 GeV. The measurement of the spin-asymmetry for the production of correlated charge conjugated hadrons of opposite transverse momentum can be directly related to $\Delta G(\eta)$ through the photon-gluon fusion process. We also present a numerical analysis of the accuracy which can be obtained for different flavors and kinematics of the observed hadron pair.

PACS numbers: 13.60.Hb, 13.88.+e, 13.87.Ce

* corresponding author: a.bravar@cern.ch

† On leave from Yerevan Physics Institute, 375036 Yerevan, Armenia, and JINR, 141980 Dubna, Russia

1 Introduction

Polarized deep inelastic scattering (DIS) experiments have shown that the quark spins account for only a rather small fraction of the nucleon spin [1], thus implying an appreciable contribution either from gluon spins or possibly from orbital angular momentum. Competing explanations exist for this result, in which the polarized glue ΔG or the negatively polarized strange quarks Δs lower the quark contribution to the nucleon spin. One way to solve this puzzle is to measure ΔG directly by studying, for example, polarized semi-inclusive processes, where the gluons enter in the initial state of the hard scattering sub-processes at lowest order in α_s .

Since the main hard scattering sub-process in DIS is the virtual photo-absorption $\gamma^* q \rightarrow q$ (q -event, fig. 1a), the measurement of inclusive polarized structure functions, like $g_1(x)$, does not allow the separation of the various parton components, and does not give direct access to the spin-dependent gluon distribution $\Delta G(\eta)$. In principle, the integral $\Gamma = \int \Delta G(\eta) d\eta$ can be extracted indirectly from the QCD analysis of the Q^2 dependence of $g_1(x, Q^2)$ [2]. Information on the shape of ΔG , however, can only be obtained from a direct measurement, which is in any case highly desirable. At first order in α_s two hard sub-processes, the gluon radiation (qg -event, fig. 1b) and the photon-gluon fusion ($q\bar{q}$ -event, fig. 1c) contribute to the DIS cross section. These QCD effects are not only clearly visible as $(2 + 1)$ jets at the Hera Collider [3], but also in the event shapes and transverse momentum spectra of hadrons produced in DIS at typical fixed target energies of 100 – 500 GeV [4]. The unpolarized gluon distribution has been also extracted in a fixed target DIS experiment from the event shape analysis of the events [5].

Favorable conditions to measure $\Delta G(\eta)$ are given, for example, in heavy flavor production [6] which proceeds via photon-gluon fusion (PGF), and in the reaction $\gamma^* + N \rightarrow 2$ high- p_T jets + X [7] which also proceeds via PGF (fig. 1c), however with a non-negligible background from gluon radiation (fig. 1b). The latter measurement requires the detection of two jets with large transverse momenta ($p_T(\text{jet}) > 5$ GeV/ c). At the moderate energies of fixed target experiments the criteria for identifying jets are not unambiguous (this is the case also at collider energies) due to their large angular spread and low particle multiplicity. On the other hand, leading hadrons produced in DIS reflect the original parton direction and flavor. The detection of these hadrons or *pseudo* jets allows to tag the partons emerging from the hard sub-processes of figs. 1b and 1c. This is also valid for fixed target experiments with typical incident lepton energies of 200 GeV.

We propose to look for two correlated high- p_T hadrons, h_1 and h_2 , in the forward hemisphere ($x_F > 0$) with $p_T(h_1) > p_{T,min}$ and h_2 opposite in azimuth to h_1 with $p_T(h_2) > p_{T,min}$. The measured cross section spin-asymmetry for $h_1 + h_2$ production can be related to the gluon polarization $\Delta G(\eta)$. For high enough p_T 's soft contributions to the $h_1 + h_2$ cross section are small, so only the hard part (figs. 1b and 1c) contributes significantly to the cross section. From the study of this process a $p_{T,min} > 1.0 - 1.5$ GeV/ c is found to be sufficiently large to suppress almost completely the contribution of the leading order sub-process (fig. 1a) to the $h_1 + h_2$ cross

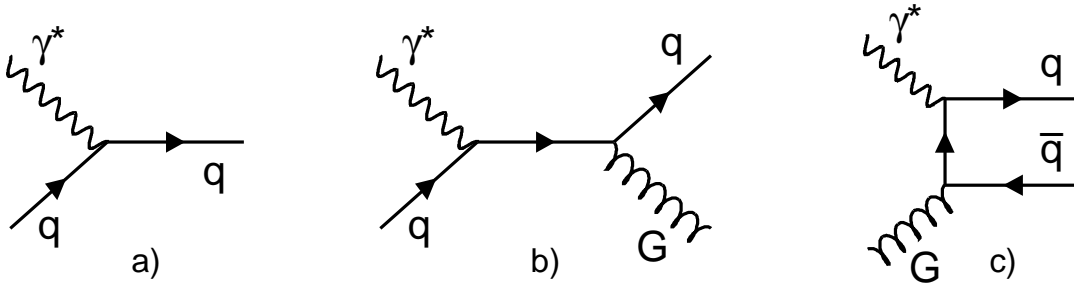


Figure 1: Lowest order Feynman diagrams for DIS $\gamma^* N$ scattering: a) virtual photo-absorption, b) gluon radiation (Compton diagram), c) photon-gluon fusion (PGF).

section. We will also consider the production of such hadron pairs in the photo-production limit using the full virtual photon spectrum down to quasi-real photons.

When developing these ideas we have found that similar arguments have been proposed previously [8] but not to the extent given here and without a quantitative analysis and without predictions. Proposals to measure ΔG by detecting a single high- p_T hadron accompanied by a second fast hadron with a large longitudinal momentum have been also made [9]. In this case a very large p_T cut-off of about 3 to 4 GeV/ c is required to select the processes of figs. 1b and 1c which considerably reduces the event yields.

2 Electro-production of high- p_T hadrons

Factorization allows the decomposition of the (polarized) electro-production cross section up to the first nontrivial order in pQCD for the production of high- p_T hadron pairs ($h_1 + h_2$) as

$$(\Delta)\sigma^{h_1+h_2} = \sum_q \left\{ (\Delta)q \otimes (\Delta)\hat{\sigma}^{\gamma^* q \rightarrow q} \otimes D_q^{h_1+h_2} \right\} + \quad (1a)$$

$$\sum_q \left\{ (\Delta)q \otimes (\Delta)\hat{\sigma}^{\gamma^* q \rightarrow qG} \otimes D_{q,G}^{h_1+h_2} \right\} + \quad (1b)$$

$$\sum_q \left\{ (\Delta)G \otimes (\Delta)\hat{\sigma}^{\gamma^* G \rightarrow q\bar{q}} \otimes D_{q,\bar{q}}^{h_1+h_2} \right\}. \quad (1c)$$

The decomposition reflects the processes shown in fig. 1. The convolutions (\otimes) are performed over the hard scattering kinematics, the (polarized) quark ($\Delta)q$ and gluon ($\Delta)G$ distributions, and the fragmentation functions involved. The sums \sum_q run over the (anti)quark flavors. $(\Delta)\hat{\sigma}^{\gamma^* q \rightarrow q}$, $(\Delta)\hat{\sigma}^{\gamma^* q \rightarrow qG}$, and $(\Delta)\hat{\sigma}^{\gamma^* G \rightarrow q\bar{q}}$ are the (polarized) partonic hard-scattering cross sections for the zero order q -event, and the first order α_s qg - and $q\bar{q}$ -events, respectively ¹. D_q , $D_{q,G}$, and $D_{q,\bar{q}}$ describe the fragmentation of partons to $h_1 + h_2$. As long as the polarization of the final hadronic state is not studied they are spin-independent. For more details see for instance [10].

¹At present, the unpolarized cross sections are calculated to next to leading order, while the polarized ones to leading order only. For their exact leading order expressions see [14, 10].

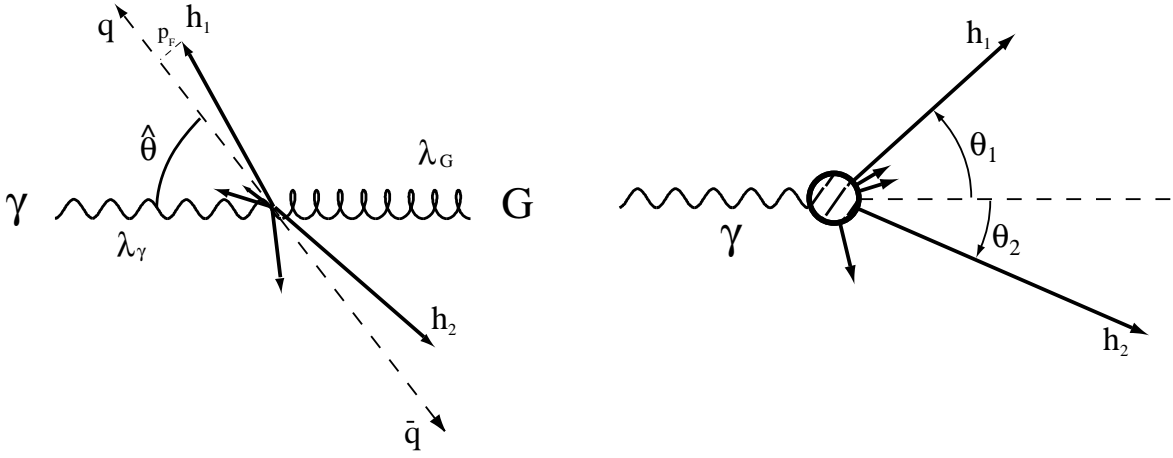


Figure 2: Correlated high- p_T hadron production as seen in the γ^* - parton c.m. (left) and in the laboratory (right). The two frames are related by a Lorentz boost with $\gamma = E_{\gamma^*}/\sqrt{\hat{s}}$.

The cross sections in eqn. 1 exhibit collinear divergencies since the α_s order QCD amplitudes for $\hat{\sigma}^{\gamma^* q \rightarrow qg}$ and $\hat{\sigma}^{\gamma^* g \rightarrow q\bar{q}}$ are divergent in the t channel the first ($\cos \hat{\vartheta} \rightarrow -1$, where $\hat{\vartheta}$ is the c.m. angle between the incoming γ^* and the outgoing quark) and in the t and u channels the latter ($\cos \hat{\vartheta} \rightarrow \mp 1$). To avoid these singularities in a Monte Carlo simulation procedure some cut-offs on the matrix elements are usually imposed. The choice, however, is not unique [11]. In our case the selection of correlated *pseudo* jets with large p_T 's implies that most of the c.m. energy of the hard sub-process $\sqrt{\hat{s}}$ goes to the outgoing parton transverse momenta \hat{p}_T , and that the outgoing partons are produced close to $\hat{\vartheta} = \pm 90^\circ$ in the c.m., therefore far away from the kinematical regions with these collinear divergencies, where also the higher order corrections are presumably larger. This criterion is basically equivalent to the $z - \hat{s}$ scheme used to regulate the divergencies in the matrix elements [11]. The most natural scales for the studied process are the transverse momenta \hat{p}_T of the outgoing partons in the c.m.. Typically, they are chosen to be $\sum \hat{p}_T^2$ and varied between $\frac{1}{2}$ and 2 times this value.

The parton distribution functions (PDF's) in qg - and $q\bar{q}$ -events are probed at a momentum fraction

$$\eta = (\hat{s} + Q^2)/2ME_{\gamma^*} = x_{Bj} (\hat{s}/Q^2 + 1) \quad (2)$$

where E_{γ^*} is the energy of the virtual photon, and M the nucleon mass (note that $\eta \geq x_{Bj}$). With a typical lepton beam energy of 200 GeV these PDF's can be accessed in the region $\eta > 0.02$. As far as the spin of the nucleon is concerned, that appears to be the most interesting region, since the largest contribution to $\Gamma = \int \Delta G(\eta)d\eta$ is expected to come from this region [2]. The proposed method will probe the PDF's at a scale $\gtrsim 10 \text{ GeV}^2$.

Next we examine the fragmentation process to high p_T hadrons (relative to the virtual photon axis). This is a non-perturbative process for which we have no detailed predictions and at present can be tackled only via a model approach by using, for instance, the observed hadron spectra to parametrize the fragmentation functions (FF's). In the fragmentation process hadrons acquire some transverse momentum, p_F , with respect to the initial quark direction,

which in the LUND string model is usually parametrized with a gaussian distribution with $\langle p_F \rangle \sim 0.36$ GeV/ c and a harder tail at the one percent level [12]. Hadrons acquire also part of their transverse momentum p_T from the intrinsic transverse momentum, k_T , of the partons in the nucleon ($p_T \sim z \cdot k_T$, where z is the fraction of the parton energy carried by the hadron). The intrinsic k_T is also parametrized with a gaussian distribution with $\langle k_T \rangle \sim 0.44$ GeV/ c . For hadrons emerging from \mathbf{q} -events these are the only sources of transverse momentum, and the resulting p_T drops off exponentially with $\langle p_T^2 \rangle \sim \langle p_F^2 \rangle + z^2 \langle k_T^2 \rangle$. The experimental data at low p_T are well reproduced by this description [13]. For example, the fraction of \mathbf{q} -events with at least one hadron with $p_T > 1.5$ GeV/ c is of the order $< 10^{-3}$.

In contrast to this scenario, the p_T spectra of hadrons emerging from events with an underlying first order QCD sub-process show a power law dependence and hence fall off much more slowly as seen in the experimental data [13]. In this case a considerable fraction of p_T comes from the transverse momentum \hat{p}_T of the outgoing partons, and the intrinsic p_F and k_T will have only a minor effect on the p_T 's of the leading hadrons, provided that the p_T is sufficiently large. So the direction of these hadrons in the partonic c.m. will approximately be that of the fragmenting partons (see fig. 2). A cut-off of $p_{T,min} > 2$ GeV/ c should be already sufficient to start suppressing the \mathbf{q} -events in the single hadron p_T spectra. Higher values for $p_{T,min}$ in excess of 3 – 4 GeV/ c would be preferable. Such a high value for the p_T cut-off, however, reduces significantly the event yields. For two high- p_T hadrons opposite in azimuth, instead, a considerably lower $p_{T,min}$ cut-off is sufficient to suppress the \mathbf{q} -events. If \hat{p}_T is large enough ($\hat{p}_T > 2$ GeV/ c), one would expect that the two outgoing partons will fragment independently into hadrons. In this case the FF's $D_{q,G}^{h_1+h_2}$ and $D_{q,\bar{q}}^{h_1+h_2}$ to two high- p_T hadrons in eqns. 1b and 1c represent indeed a product of two one-particle FF's: $D_{q,G}^{h_1+h_2} = D_q^{h_1} \times D_G^{h_2} + (1 \leftrightarrow 2)$ and $D_{q,\bar{q}}^{h_1+h_2} = D_q^{h_1} \times D_{\bar{q}}^{h_2} + (1 \leftrightarrow 2)$.

3 The Asymmetry and $\Delta G/G$

The polarized electro-production cross section spin-asymmetry $A_{LL}^{lN \rightarrow h_1 h_2}$ at order α_s can be written as

$$A_{LL}^{lN \rightarrow h_1 h_2} = \frac{\sum_q \left\{ \Delta G \otimes \Delta \sigma^{\gamma^* G \rightarrow q \bar{q}} \otimes D_{q,\bar{q}}^{h_1+h_2} \right\} + \sum_q \left\{ \Delta q \otimes \Delta \sigma^{\gamma^* q \rightarrow q G} \otimes D_{q,G}^{h_1+h_2} \right\}}{\sum_q \left\{ G \otimes \sigma^{\gamma^* G \rightarrow q \bar{q}} \otimes D_{q,\bar{q}}^{h_1+h_2} \right\} + \sum_q \left\{ q \otimes \sigma^{\gamma^* q \rightarrow q G} \otimes D_{q,G}^{h_1+h_2} \right\}}. \quad (3)$$

The notation is as in eqn. 1. The virtual photon depolarization with respect to the incident muon polarization has been absorbed into the polarized cross sections. The contribution to $A_{LL}^{lN \rightarrow h_1 h_2}$ from the leading order diagram (fig. 1a) is strongly suppressed when selecting high- p_T correlated hadron pairs (see next section), and therefore it has not been included in eqn. 3. On the other hand, the spin-asymmetry for the leading order sub-process is very small in the relevant kinematical range, and at most would introduce a small dilution in $A_{LL}^{lN \rightarrow h_1 h_2}$.

Two competing sub-processes of the same order in α_s contribute to the (polarized) cross section and $A_{LL}^{lN \rightarrow h_1 h_2}$. Only the PGF, however, is of interest for the extraction of the (polarized)

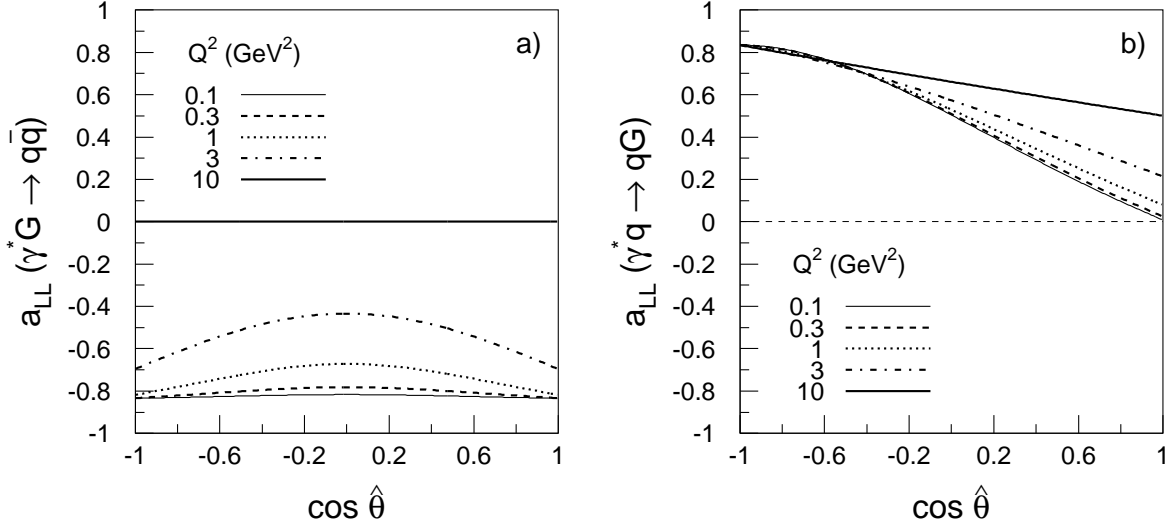


Figure 3: Basic scattering asymmetries \hat{a}_{LL} for the photon-gluon fusion (a) and the gluon radiation (b) as a function of the c.m. scattering angle $\hat{\vartheta}$ for different values of Q^2 at fixed $\hat{s} = 10 \text{ GeV}^2$ and fixed $y = 0.7$ ($D \approx 0.83$). Note their Q^2 dependence.

gluon distribution $(\Delta)G(\eta)$, while the Compton process acts as a background. To quantify this contribution we introduce the ratio

$$R = \frac{\sigma^{PGF}}{\sigma^{COMPT}} = \frac{\sum_q \left\{ G \otimes \hat{\sigma}^{\gamma^* G \rightarrow q\bar{q}} \otimes D_{q,\bar{q}}^{h_1+h_2} \right\}}{\sum_q q \left\{ \otimes \hat{\sigma}^{\gamma^* q \rightarrow qG} \otimes D_{q,G}^{h_1+h_2} \right\}} \propto \frac{G(\eta)}{F_1(\eta)}, \quad (4)$$

which depends in particular on the covered η region. The Compton background is proportional to the unpolarized structure function F_1 , and over the covered kinematical region it is dominated by scattering off *u-valence* quarks because of their large charge compared to other quark flavors and large density compared to *sea* quarks.

For a qualitative discussion of the asymmetry $A_{LL}^{LN \rightarrow h_1 h_2}$, showing explicitly the contributions of different processes, eqn. 3 can be approximated as

$$A_{LL}^{LN \rightarrow h_1 h_2} \approx \langle \hat{a}_{LL}^{\gamma^* G \rightarrow q\bar{q}} \rangle \frac{\Delta G}{G} \frac{R}{1+R} + \langle \hat{a}_{LL}^{\gamma^* q \rightarrow qG} \rangle A_1 \frac{1}{1+R}. \quad (5)$$

A_1 is the virtual photo-absorption asymmetry, and the $\langle \hat{a}_{LL} \rangle$'s are the scattering asymmetries at partonic level ($\hat{a}_{LL} = \Delta \hat{\sigma} / \hat{\sigma}$). At present they are calculated to order α_s only [14]. Figure 3 shows these asymmetries for the two sub-processes considered above as a function of the c.m. scattering angle $\hat{\vartheta}$ for different values of the photon virtuality Q^2 at fixed $\hat{s} = 10 \text{ GeV}^2$ and fixed $y = 0.7$ ($y \approx E_{\gamma^*} / E_{beam}$) to which corresponds a depolarization D of about 83 %. For most of the proposed measurement the PGF asymmetry $\hat{a}_{LL}^{\gamma^* G \rightarrow q\bar{q}}$ (fig. 3a) is close to $-1 \times D$. The asymmetry $\hat{a}_{LL}^{\gamma^* q \rightarrow qG}$ for the Compton process (fig. 3b) instead is always positive and close to $+0.5 \times D$ for scattering at 90° in the c.m.. The two sub-processes, therefore, contribute with opposite signs and weights to $A_{LL}^{LN \rightarrow h_1 h_2}$. Since $|\langle \hat{a}_{LL}^{\gamma^* G \rightarrow q\bar{q}} \rangle|$ is about 2 times as large as $|\langle \hat{a}_{LL}^{\gamma^* q \rightarrow qG} \rangle|$, and the asymmetries of the relevant backgrounds are proportional to A_1 , which is rather small in the relevant range [1], this process offers favorable conditions for the measurement of $\Delta G(\eta)$.

In order to extract the gluon polarization from the measured asymmetry $A_{LL}^{LN \rightarrow h_1 h_2}$ one assumes that the leading order contribution is negligible and subtracts the contribution of the Compton sub-process (fig. 1b) from eqn. 3. The quark polarizations $\Delta\mathbf{q}$ over the relevant range are already available from other measurements [15]. These backgrounds (proportional to A_1), reduce to a dilution effect when using isoscalar targets, because for such target materials A_1 is very small (close to zero) in the relevant kinematical range [1]. The ratio $R = \sigma^{PGF}/\sigma^{COMPT}$ can be estimated from simulations of this process, but not measured directly. The incomplete knowledge of R will introduce the largest uncertainty in the extraction of $\Delta G/G$. Therefore it is important to maximize this ratio by selecting, for instance, specific configurations in the final state as discussed in the next section and get reliable and stable predictions for it.

4 Tagging the PGF

We have studied the electro-production of two high- p_T hadrons described above using existing event generators [16, 17, 18], which contain all the relevant underlying physics processes including the exact treatment of the α_s first order matrix elements (fig. 1) and are known to reproduce fairly accurately the final hadronic state in a variety of processes, including the observed p_T and p_L hadron spectra, the angular distributions, the measured cross sections, etc.. We performed our quantitative analysis in the kinematical conditions of the COMPASS experiment [23] for a 200 GeV/c μ^+ beam incident on a deuteron (iso-scalar) target with $0.5 < y < 0.9$ ($100 < E_{\gamma^*} < 180$ GeV) and $W^2 > 200$ GeV². A slightly modified version of the electro-production LEPTO [16] event generator has been used down to $Q^2 = 0.4$ GeV² with the leading order unpolarized parton densities of [19]. Different descriptions of the fragmentation process within the LUND model [12, 18] (string fragmentation or independent fragmentation) have been considered including the color dipole model of [17]. They all give results consistent with each other. We also varied several settings in the generators in order to verify the stability of the results.

The following selections of the high- p_T hadron pairs, based on the discussions in the previous section and the results of the simulations, are found to enhance the relative contributions of the $q\bar{q}$ - and qg -events over the q -events.

A – p_T cut: There should be two hadrons in the event with $p_T > 1.0 - 1.5$ GeV/c. Since $\sqrt{\hat{s}} > m(h_1, h_2)$, where $m(h_1, h_2)$ is the invariant mass of the $h_1 + h_2$ pair, we also demand that $m(h_1, h_2) > 2.5 - 3.0$ GeV/c² in order to impose a lower limit on the c.m. energy $\sqrt{\hat{s}}$. The final event yields depend sensitively on these cuts; they will be chosen to obtain the best compromise of statistical and systematical accuracies.

B – x_F cut: To avoid fragmentation effects from the target remnant only hadrons produced in the forward hemisphere with $x_F > 0$ should be considered, which corresponds to a cut $z > 0.1$ for each selected hadron.

C – $\Delta\phi$ cut: The two hadrons should be found opposite in azimuth, such that $|\Delta\phi| = 180^\circ \pm 30^\circ$,

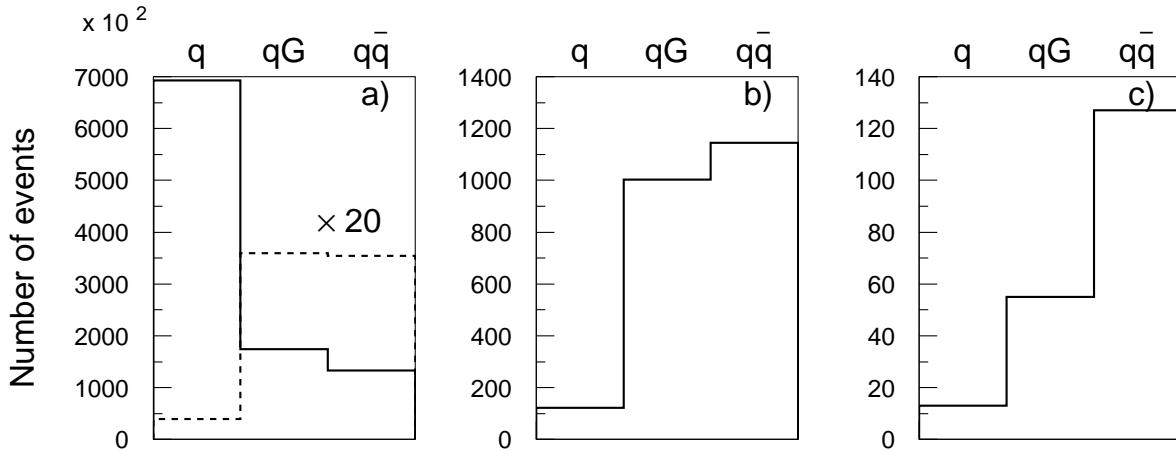


Figure 4: Contributions of different sub-processes to the cross section: (a) no cuts (full line) and selected hadron pairs (cuts **A** to **C**, dashed line); (b) oppositely charged hadron pairs; (c) oppositely charged kaon pairs. The event yields are normalized to 10^6 generated events.

where ϕ is the azimuthal angle between the lepton scattering plane and outgoing hadron. Conservation of p_T already introduces a strong correlation, if primordial k_T and higher order α_s contributions are small.

As can be observed from fig. 4a, these selections are already strong enough to enhance the relative contributions of the $q\bar{q}$ - and qg -events over the q -events (dashed vs. full line). Further, the relative contribution of the PGF over the Compton sub-process can be enhanced as follows. **D – oppositely charged hadrons:** Fragmenting partons in $q\bar{q}$ -events have opposite charges and favored fragmentation will preferentially lead to oppositely charged leading hadrons in contrast to qg -events, where the gluon fragments with equal probability to positive and negative hadrons. Therefore selecting events with oppositely charged hadrons will enhance the contribution of the $q\bar{q}$ -events over the qg -events.

E – K^+K^- pairs: The production of strange hadrons in fragmentation is suppressed compared to non-strange hadrons, unless there is already an s quark in the initial state. This effect is parametrized with a strangeness suppression factor γ_s , which presently ranges between 0.2 and 0.3 [20]. The production of a high p_T correlated kaon pair will be therefore strongly suppressed, unless there is already a fragmenting $s\bar{s}$ pair. This selection, however, reduces the event yields by about a factor of 10.

Figures 4b and 4c show the relative suppression of the q -events for oppositely charged hadron and kaon pairs ², respectively, compared to fig. 4a (full line) where no selections on the final hadronic state have been applied. The selections for the hadron pairs shown in fig. 4b are **A** to **D** and for the kaon pairs of fig. 4c **A** to **E** with $p_T > 1.0$ GeV/ c and $m(h^+, h^-) > 2.5$ GeV/ c^2 . We will use the same cuts also in the following. The fraction of q -events in both selected samples is around 5 %. The relative contribution of the $q\bar{q}$ -events over the qg -events R (eqn. 4)

²A hadron pair can consist also of hadrons of different flavors. The sample of kaon pairs forms a subset in the sample of hadron pairs.

over the whole covered kinematical range is about 1 for the selected $h^+ + h^-$ pairs and about 2 for the selected $K^+ + K^-$ pairs (see also figs. 5a and 5b from where the η dependence of R can be inferred). The reduction factors r of the event rates are $r^{h^+h^-} \sim 2.4 \times 10^{-3}$ and $r^{K^+K^-} \sim 2.2 \times 10^{-4}$, respectively. The large event yields in the $h^+ + h^-$ channel also allow one to apply tighter selections for this sample such as $p_T > 1.5 \text{ GeV}/c$, for which $r^{h^+h^-} \sim 2.6 \times 10^{-4}$. These results have been obtained with the LEPTO program [16] with the kinematical settings as discussed above.

We have also considered the production of the correlated high- p_T hadron pairs in the photo-production limit, because the total cross section, and correspondingly the event yields, are substantially increased in the $Q^2 \rightarrow 0$ limit. As already mentioned, the relevant scales for the studied process are set by the scale of the hard sub-processes $\sum \hat{p}_T^2$, and are around or above 10 GeV^2 . We have studied the photo-production limit with the photo-production event generator PYTHIA [18]. We have obtained results very close to the ones given above for the electro-production case with $Q^2 > 0.4 \text{ GeV}^2$ ($Q^2 > 1 \text{ GeV}^2$). Also the contribution from non-pointlike photons has been found to be small. We therefore assume the same results to hold over the Q^2 region not covered with the simulation extending from $Q^2 = 0.4 \text{ GeV}^2$ ($Q^2 > 1 \text{ GeV}^2$) to $Q_{min}^2 = m_\mu^2 \frac{E_\gamma^{*2}}{E_{beam}(E_{beam} - E_\gamma^*)}$, where Q_{min}^2 is determined from the energy-momentum conservation at the lepton vertex. The estimated cross section for producing such hadron pairs $\sigma^{lN \rightarrow h^+h^-}$ ($\sigma^{lN \rightarrow K^+K^-}$) is around $(150 \pm 50) \text{ nb} \times r^{h^+h^-}$ ($r^{K^+K^-}$). This result has been obtained by extrapolating the DIS cross section from $Q^2 > 0.4 \text{ GeV}^2$ ($Q^2 > 1 \text{ GeV}^2$) to Q_{min}^2 using a dipole form factor with a mass parameter of 10 GeV^2 set by the scale of the hard process. This procedure is similar to that adopted for extracting the open charm and J/Ψ photo-production cross section from the measured muo-production cross sections [21].

Figure 5 shows the η distributions of the partons (quarks and gluons) for the selected high- p_T hadron and kaon pair samples. The shapes result from the combined effect of the chosen photon energy and the general behavior of the parton distributions. The η distribution is peaked around 0.1. For the h^+h^- sample the \mathbf{qg} -events dominate over $\mathbf{q\bar{q}}$ -events above $\eta \sim 0.15 - 0.20$, while for the K^+K^- sample the relative contribution of the \mathbf{qg} - and $\mathbf{q\bar{q}}$ -events are similar above the same η . The accessible gluon η region extends from $\eta \sim 0.02$ to $\eta \sim 0.2$ for a 200 GeV beam.

Assuming that in the hard scattering c.m. the directions of the selected hadrons are approximately that of the outgoing partons we can try to reconstruct the hard scattering kinematics using the two measured hadrons only. Neglecting the fragmentation p_F , the longitudinal (\hat{p}_L) and the transverse (\hat{p}_T) momentum components of the *pseudo* jet in the partonic c.m. can be written as

$$\hat{p}_L = \xi \hat{p} \cos \hat{\vartheta} \quad \text{and} \quad \hat{p}_T = \xi \hat{p} \sin \hat{\vartheta} \quad (6)$$

where $\hat{p} = \sqrt{\hat{s}}/2$ is the total momentum of the parton. ξ represents the energy fraction of the original parton carried away by the hadron. The c.m. angle $\hat{\vartheta}$ is then related to the laboratory

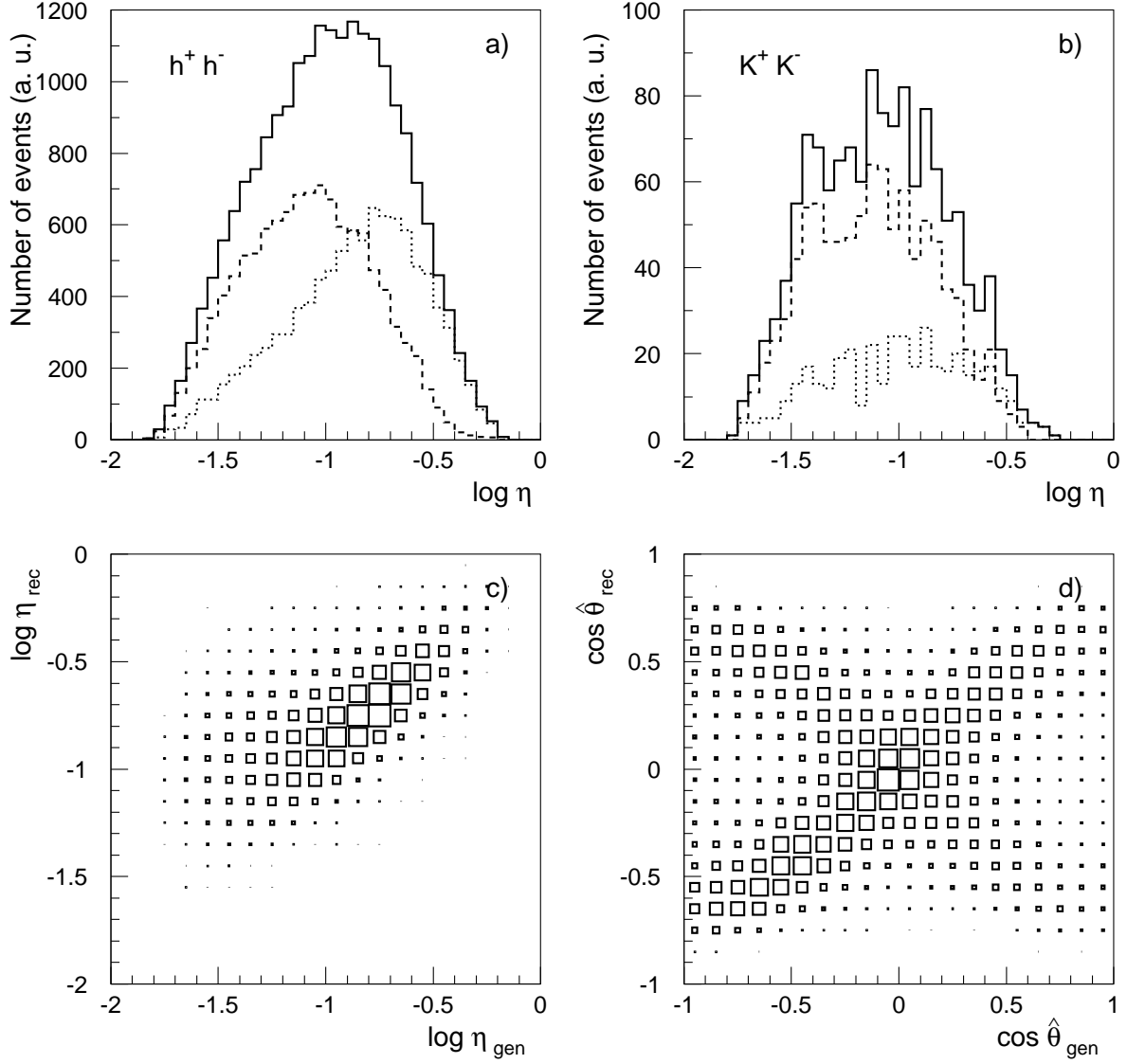


Figure 5: η distributions of the gluons ($q\bar{q}$ -events dashed line) and of the quarks (qg -events dotted line) for the selected high- p_T hadron pairs (a) and kaon pairs (b). The full line is the sum of the two. Correlations between the generated and the reconstructed parton momentum fraction η (c) and the scattering c.m. angle $\cos \hat{\vartheta}$ (d) using the kinematics of the two selected hadrons only.

angle ϑ_{LAB} between the virtual photon axis and the hadron direction by

$$\tan \vartheta_{LAB}^{\pm} = \frac{p_T}{p_L} = \frac{\sin \hat{\vartheta}}{\gamma (1 \pm \cos \hat{\vartheta})} \quad (7)$$

where $\gamma = E_{\gamma^*}/\sqrt{\hat{s}}$ is the Lorentz boost factor. The \pm sign refers to h^+ and h^- , respectively. We can also obtain the c.m. energy \hat{s} from the measured angles ϑ_{LAB}^+ and ϑ_{LAB}^- for the selected positive and negative hadron as:

$$\hat{s} = E_{\gamma^*}^2 \tan \vartheta_{LAB}^+ \tan \vartheta_{LAB}^- . \quad (8)$$

The parton momentum fraction η follows from eqn. 2. The c.m. scattering angle $\hat{\vartheta}$, instead, is obtained from

$$\cos \hat{\vartheta} = \frac{\tan \vartheta_{LAB}^+ - \tan \vartheta_{LAB}^-}{\tan \vartheta_{LAB}^+ + \tan \vartheta_{LAB}^-} . \quad (9)$$

A rather good correlation between the generated momentum fraction η_{gen} and the reconstructed one η_{rec} can be observed in fig. 5c, which will allow us also to study $\Delta G/G$ as a function of η . Figure 5d shows the correlation between the scattering c.m. angle $\cos \hat{\vartheta}_{gen}$ and the reconstructed one $\cos \hat{\vartheta}_{rec}$. The generated $\cos \hat{\vartheta}_{gen}$ is defined with respect to the outgoing quark for both the qg - and $q\bar{q}$ -event, and the reconstructed $\cos \hat{\vartheta}_{rec}$ is calculated with respect to the positive hadron. This explains the double structure of the plot, since a quark can fragment also to a negative hadron ($s \rightarrow K^-$). These correlations also demonstrate the charge retention in the process and that the kinematics of the high- p_T hadron pair is strongly correlated with the kinematics of the outgoing partons in the c.m. (eqn. 6).

By selecting, for instance, hadron pairs with $|\cos \vartheta_{rec}| < 0.5$, we will select events with $\hat{\vartheta}$ even closer to 90° in the hard scattering c.m.. Since the Compton sub-process is peaked in the backward direction ($\cos \hat{\vartheta} \rightarrow -1$), this additional cut will further suppress the qg -events and therefore enhance the relative contribution of the $q\bar{q}$ -events. Another possibility would be to require $x_F^- > x_F^+$, since the Compton sub-process will preferentially generate faster positive hadrons because of the favored fragmentation of u quarks to positive hadrons.

5 The Results

Figure 6 shows the cross section spin-asymmetries $A_{LL}^{LN \rightarrow h^+h^-}$ and $A_{LL}^{LN \rightarrow K^+K^-}$ as a function of η_{gen} for the selected charged hadron pairs (selections **A** to **D**) and the kaon pairs (selections **A** to **E**) obtained by integrating eqn. 3 with the POLDIS program [14] and using different polarized parton densities from [22] (sets A and C). The corresponding models for the gluon polarization $\Delta G/G$ at a scale of 10 GeV^2 are shown in fig. 6d. For the set A parametrization of the polarized parton densities, the asymmetry $A_{LL}^{LN \rightarrow h^+h^-}$ for the hadron pairs (figs. 6a and 6c) is as large as -15% just below $\eta \sim 0.1$ and then slowly decreases, in magnitude, with increasing η with a zero crossing around $\eta \sim 0.2 - 0.3$. The behavior of the asymmetry can be easily understood from the shape of $\Delta G/G$ and the contribution of the Compton sub-process over this η interval:

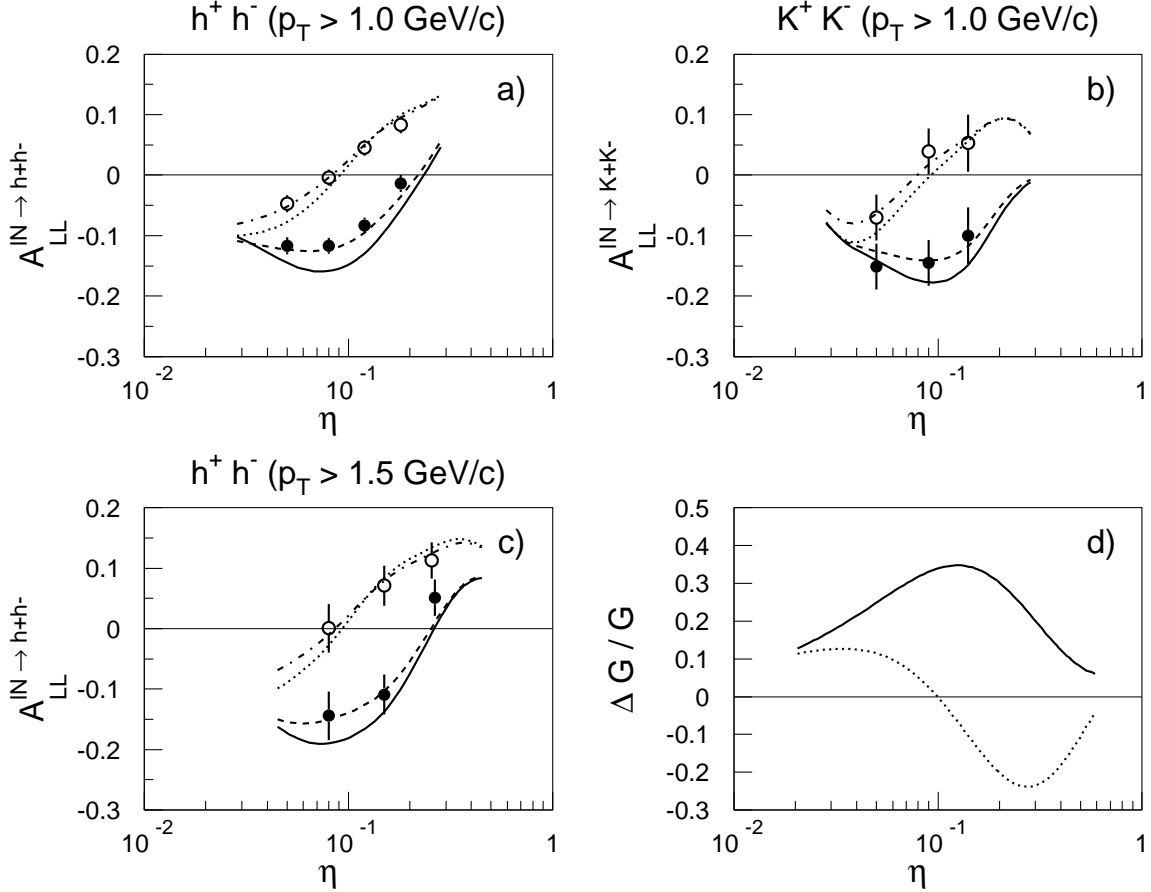


Figure 6: Cross section spin-asymmetries $A_{LL}^{lN \to h^+h^-}$ ($p_T > 1$ GeV/c) (a), $A_{LL}^{lN \to K^+K^-}$ ($p_T > 1$ GeV/c) (b), and $A_{LL}^{lN \to h^+h^-}$ ($p_T > 1.5$ GeV/c) (c) as a function of η_{gen} with the polarized parton densities of [22] (set A - full line, set C - dotted line). The circles show the same asymmetries as a function of η_{rec} (set A - full circles, set C - open circles) and the error bars indicate the relative statistical precision for the measurement obtainable in one year. The *smearing* of the asymmetry due to the finite width of the η_{rec} bins (see text) is also shown (dashed and dot-dashed lines). Also shown are the different parametrizations for the gluon polarization $\Delta G/G$ used at a scale of 10 GeV 2 (d).

the Compton sub-process contributes to $A_{LL}^{lN \rightarrow h^+h^-}$ with a sign opposite to that for the PGF and its relative contribution increases with increasing η . For the set C the zero crossing occurs at a lower value of η around 0.1, reflecting the fact that $\Delta G/G < 0$ here (fig. 6d). The asymmetry for the selected K^+K^- pairs (fig. 6b) shows a similar behavior as a function of η . It reaches a maximum value of almost -20% for η just below 0.1 for set A. The relative contribution of the Compton sub-process for this sample is smaller, and the expected asymmetry is therefore larger. The photo-production asymmetries $A_{LL}^{\gamma N \rightarrow h^+h^-}$ and $A_{LL}^{\gamma N \rightarrow K^+K^-}$ can be obtained from the electro-production ones by dividing the latter ones with the depolarization factor D , which is around 80% .

Using the correlation between the generated and reconstructed parton momentum fraction η_{gen} and η_{rec} shown in fig. 5c, we can divide the high- p_T hadron pairs in several η_{rec} bins and study $A_{LL}^{lN \rightarrow h^+h^-}$ ($A_{LL}^{lN \rightarrow K^+K^-}$) as a function of η_{rec} . In fig. 6 these asymmetries for several η_{rec} bins are also shown. Because of the finite width of the correlation between η_{gen} and η_{rec} , each η_{rec} bin covers a slightly larger η_{gen} interval, which explains the small discrepancies observed between the asymmetries plotted as a function of η_{gen} and η_{rec} . This *smearing* of the asymmetry can be easily reproduced by introducing a smearing in η_{gen} for $A_{LL}^{lN \rightarrow h^+h^-}$ ($A_{LL}^{lN \rightarrow K^+K^-}$) as shown in the same plots (fig. 6). Nevertheless the asymmetries calculated at the partonic level survive the hadronization phase well, allowing one also to distinguish easily between different parametrizations for $\Delta G/G$.

In a high rate fixed target experiment like COMPASS [23], integrated luminosities L of 2 fb^{-1} can be achieved in one year. With the cross section $\sigma^{lN \rightarrow h^+,h^-} = 150 \text{ nb} \times r^{h^+,h^-}$ for producing a high- p_T hadron pair as discussed in the previous section, about 700 k h^+h^- pairs (cuts **A** to **D**) and about 70 k K^+K^- pairs (cuts **A** to **E**) with $p_T > 1 \text{ GeV}/c$, and about 80 k h^+h^- pairs with $p_T > 1.5 \text{ GeV}/c$ can be collected. Given a beam polarization P_B of $\sim 80\%$ and an effective target polarization P_T of $\sim 25\%$ per nucleon, which includes the dilution factors, these event samples will give a statistical precision in the 1% region for both $A_{LL}^{lN \rightarrow h^+h^-}$ and $A_{LL}^{lN \rightarrow K^+K^-}$ spin-asymmetries. Note that the measured (*raw*) asymmetry $\varepsilon_{LL}^{lN \rightarrow h^+h^-} = P_B \times P_T \times A_{LL}^{lN \rightarrow h^+h^-}$ is about 3–4 times smaller. In figure 6 the expected accuracies for the data divided in several η_{rec} bins are also shown.

As already discussed, in order to extract $\Delta G/G$ from $A_{LL}^{lN \rightarrow h^+h^-}$ ($A_{LL}^{lN \rightarrow K^+K^-}$) the various backgrounds have to be subtracted from the asymmetries (eqn. 5). Simulations have shown that the ratio $R = \sigma^{PGF}/\sigma^{COMPT}$ is rather stable with variations contained to within 10% to 15% of its value for different descriptions of the fragmentation process and various parametrizations of the unpolarized parton densities. The polarized quark densities $\Delta \mathbf{q}/\mathbf{q}$ are already known with a rather good precision of about 10% [15], and are expected to improve in the near future. Assuming a rather generous error of 20% for R and 10% for $\Delta \mathbf{q}/\mathbf{q}$, we have estimated a statistical and systematical precision of about 5% for $\Delta G/G$ from the measured $A_{LL}^{lN \rightarrow h^+h^-}$ and $A_{LL}^{lN \rightarrow K^+K^-}$ asymmetries for each η_{rec} bin. The precision on the extraction of $\Delta G/G$ is mostly affected by the Compton background subtraction, which is larger in the h^+h^- channel

compared to the K^+K^- one, where, on the other hand, the event yields are smaller. The simultaneous use of different charge and flavor combinations, and different kinematics of the hadron pairs will give a better determination of $\Delta G/G$ because of the different backgrounds involved, while the gluon densities remain the same.

6 Conclusions

In conclusion, we have shown that the measurement of the cross section spin-asymmetry for two azimuthally anti-correlated hadrons of moderate transverse momentum p_T of 1–1.5 GeV/ c in polarized electroproduction on polarized targets offers a considerable sensitivity on the gluon polarization $\Delta G/G$ at momentum fractions η around 0.1. Current models for ΔG predict experimental asymmetries of up to 20 % (5 % with realistic dilution assumptions) and sufficiently large cross sections to achieve statistical accuracies in the 1 % region for one year of running of the COMPASS experiment.

This method should be seen as complementary to the measurement of spin asymmetries for open charm production discussed up to now [6, 23], since the systematic effects expected in the two processes are very different. The PGF process not only gives opposite signs for the asymmetry of the two processes but higher order QCD effects and hadronization effects will be very different. The new process offers the additional advantage that the parton kinematics can be, at least approximately, reconstructed from the observed hadron pairs. This will not only allow a direct measurement of the shape of $\Delta G(\eta)$ over the range 0.04 – 0.2, but also checks and corrections for model dependencies. The systematics for the ΔG determination from the hadron pairs are dominated by the poorly known fraction R of PGF events in the total sample. Usage of isoscalar targets reduces this to a dilution effect since the asymmetries of the relevant backgrounds are proportional to A_1 , which is very small in the relevant range.

Further studies, which are beyond the scope of the present paper, show that the simultaneous use of different selections of charge, flavor, and kinematics will narrow down the systematic error in the quantity R . This can be seen, for instance, from figs. 4 and 5 which show that different selections of the hadron pairs provide us with different values for R connecting the same basic quantities in eqn. 5.

Another major uncertainty stems from the use of only leading order processes in our estimates. We expect, however, that higher orders will not change the picture in a dramatic way since the relevant scales are of the order of 10 GeV², comparable to the threshold for open charm production, and that the polarization asymmetries survive gluon radiation through helicity conservation.

In summary, the observation of a negative asymmetry in the proposed measurement will be a clear signature for a non-zero positive gluon polarization. The experiment will be also sensitive to very small gluon polarizations, up to five times smaller as currently discussed models.

Acknowledgments

We would like to thank D. De Florian, K. Kurek, G.K. Mallot, and W. Vogelsang for valuable discussions.

References

- [1] EMC, J. Ashman *et al.*, Nucl. Phys. B **328**, 1 (1989); SMC, B. Adeva *et al.*, Phys. Lett. B **396**, 338 (1997); E154, K. Abe *et al.*, Phys. Rev. Lett. **79**, 26 (1995).
- [2] R.D. Ball, S. Forte, and G. Ridolfi, Phys. Lett. B **378**, 255 (1996); M. Glück *et al.*, Phys. Rev. D **53**, 4775 (1996); T. Gehrmann and W.J. Stirling, Phys. Rev. D **53**, 6100 (1996).
- [3] See for instance H1, S. Aid *et al.*, Nucl. Phys. **B449**, 3 (1995).
- [4] E665, M.R. Adams *et al.*, Phys. Rev. D **48**, 5057 (1993); EMC, M. Arneodo *et al.*, Z. Phys. C **36**, 527 (1987).
- [5] E665, M.R. Adams *et al.*, Z. Phys. C **71**, 391 (1996).
- [6] M. Glück and E. Reya, Z. Phys. C **39**, 569 (1988); for an experimental proposal see [23].
- [7] J. Feltesse, F. Kunne, and E. Mirkes, Phys. Lett. B **388**, 832 (1996).
- [8] M. Strikman, in *Internal Spin Structure of the Nucleon*, ed. by V.W. Hughes and C. Cavata (World Scientific, Singapore, 1995), p. 153.
- [9] M. Fontannaz, D. Schiff, and B. Pire Z. Phys. C **8**, 349 (1981).
- [10] R.D. Field, *Applications of Perturbative QCD*, Frontiers in Physics v. 77, Addison Wesley (1989).
- [11] J.G. Körner, E. Mirkes, and G.A. Schuler, Int. J. Mod. Phys. A **4**, 1781 (1989).
- [12] B. Andersson, G. Gustafson, G. Ingelman, and T. Sjöstrand, Phys. Rep. **97**, 31 (1983).
- [13] P. Renton and W.S.C. Williams, Ann. Rev. Nucl. Part. Sci. **31**, 193 (1981); T. Sloan, G. Smadja, and R. Voss, Phys. Rep. **162**, 45 (1988).
- [14] A. Bravar, K. Kurek, and R. Windmolders, hep-ph/9704313, to appear in Comp. Phys. Comm.
- [15] SMC, B. Adeva *et al.*, Phys. Lett. B **369**, 93 (1996).
- [16] G. Ingelman, A. Edin, and J. Rathsman, Comp. Phys. Comm. **101**, 108 (1997).
- [17] L. Lönnblad, Comp. Phys. Comm. **71**, 15 (1992).

- [18] T. Sjöstrand, *Comp. Phys. Comm.* **82**, 74 (1994).
- [19] M. Glück, E. Reya, and A. Vogt, *Z. Phys. C* **67**, 433 (1995)
- [20] E665, M.R. Adams *et al.*, *Z. Phys. C* **61**, 539 (1994); DELPHI, P. Abreu *et al.*, *Z. Phys. C* **65**, 587 (1995); ZEUS, M. Derrick *et al.*, *Z. Phys. C* **68**, 29 (1995); H1, S. Aid *et al.*, *Nucl. Phys. B* **480**, 3 (1996).
- [21] EMC, J.J. Aubert *et al.*, *Phys. Lett. B* **167**, 127 (1986).
- [22] T. Gehrmann and W.J. Stirling, *Phys. Rev. D* **53**, 6100 (1996).
- [23] The COMPASS Proposal, CERN/SPSLC 96-14, SPSC/P297, March 1996.